

The Role of Isocitrate Lyase (ICL1) in the Metabolic Adaptation of *Candida albicans* Biofilms

Oluwaseun Ayodeji Ishola,¹ Seng Yeat Ting,¹ Yasser M Tabana,¹ Mowaffaq Adam Ahmed,¹ Muhammad Amir Yunus,¹ Rafeezul Mohamed,² Leslie Thian Lung Than,³ and Doblin Sandai^{1*}

¹Infectomics Cluster, Advanced Medical and Dental Institute, Universiti Sains Malaysia, Malaysia

²Regenerative Medicine Cluster, Advanced Medical and Dental Institute, Universiti Sains Malaysia, Malaysia

³Department of Medical Microbiology and Parasitology, Faculty of Medicine and Health Sciences, Universiti Putra Malaysia, Selangor, Malaysia

*Corresponding author: Doblin Sandai, Infectomics Cluster, Advanced Medical and Dental Institute, Universiti Sains Malaysia, Malaysia. Tel: +60-45622386, Fax: +60-194951073, E-mail: doblin@usm.my, drdoblinamdiusm@gmail.com

Received 2016 March 24; Revised 2016 August 14; Accepted 2016 August 19.

Abstract

Background: A major characteristic of *Candida* biofilm cells that differentiates them from free-floating cells is their high tolerance to antifungal drugs. This high resistance is attributed to particular biofilm properties, including the accumulation of extrapolymeric substances, morphogenetic switching, and metabolic flexibility.

Objectives: This study evaluated the roles of metabolic processes (in particular the glyoxylate cycle) on biofilm formation, antifungal drug resistance, morphology, and cell wall components.

Methods: Growth, adhesion, biofilm formation, and cell wall carbohydrate composition were quantified for isogenic *Candida albicans* ICL1/ICL1, ICL1/*icl1*, and *icl1/icl1* strains. The morphology and topography of these strains were compared by light microscopy and scanning electron microscopy. *FKS1* (glucan synthase), *ERG11* (14- α -demethylase), and *CDR2* (efflux pump) mRNA levels were quantified using qRT-PCR.

Results: The ICL1/*icl1* and *icl1/icl1* strains formed similar biofilms and exhibited analogous drug-tolerance levels to the control ICL1/ICL1 strains. Furthermore, the drug sequestration ability of β -1, 3-glucan, a major carbohydrate component of the extracellular matrix, was not impaired. However, the inactivation of ICL1 did impair morphogenesis. ICL1 deletion also had a considerable effect on the expression of the *FKS1*, *ERG11*, and *CDR2* genes. *FKS1* and *ERG11* were upregulated in ICL1/*icl1* and *icl1/icl1* cells throughout the biofilm developmental stages, and *CDR2* was upregulated at the early phase. However, their expression was downregulated compared to the control ICL1/ICL1 strain.

Conclusions: We conclude that the glyoxylate cycle is not a specific determinant of biofilm drug resistance.

Keywords: Biofilms, Isocitrate Lyase (ICL1), Resistance, *Candida albicans*

1. Background

Fungal pathogens are gaining increasing attention as infection rates increase due to advances in healthcare and rising numbers of susceptible immunocompromised patients (1, 2), and their major impact on human health is becoming better appreciated. Despite advancements in the management of hospital-acquired infections, *Candida albicans*, a commensal organism that helps maintain microbiota normalcy, is the fourth most common isolated nosocomial bloodstream pathogen, after *Staphylococcus aureus*, accounting for approximately 80% of candidemia cases with a 40% fatality rate (3-9). These microbes exist predominantly as attached aggregated communities in nature, forming an irreversible assemblage that is strongly influenced by the growth medium, the attachment sur-

faces, and the environment. Microcolonies of cells are sheltered in self-secreted polymeric substances and communicate via quorum sensing (10-12).

Biofilm growth is a unique virulence trait and defense mechanism of *C. albicans* that is associated with infectious diseases and the clinical use of implanted medical devices, such as central catheters and intracardiac prosthetic valves. *Candida albicans* causes life-threatening conditions, such as urinary tract infection and endocarditis, with a mortality rate as high as 30% (10, 13, 14). Despite treatment, such an infection may re-establish itself. Sessile cells are phenotypically and genetically different from free-floating cells. A characteristic attribute of biofilms, unlike planktonics, is resistance to antifungal agents, particularly azole, polyenes, and recently, echinocandins. *Candida albicans* sessile cell resistivity is always expressed, irrespective

of definite phenotypic variation and the expression of specific drug-resistance genes, entailing complex multicellular processes (11, 15, 16). Due to this property, in most clinical cases, replacement of the infected devices is the only treatment option (13, 17, 18). Thus, it is imperative to develop effective strategies for control. Recent research has begun to shed light on how attached microbial communities develop resistance to antifungal agents, proposing various involved mechanisms (13, 14). This peculiar phenotype has been reported by previous studies to be a multifactorial phenomenon not regulated by a singular mechanism, which was confirmed by this study.

2. Objectives

In this study, we examined whether *C. albicans* biofilm development depends on the glyoxylate pathway since this is essential for the assimilation of many alternative carbon sources in the absence of glucose, and we investigated whether this pathway contributes to the high tolerance of biofilm cells to antifungal drug therapy. In addition, we examined whether a correlation exists between cell carbohydrates and matrix glucan concentrations during biofilm development.

3. Methods

3.1. Strains

Candida albicans wildtype strain ICL1/ICL1, heterozygous mutant ICL1/icl1, and homozygous mutant icl1/icl1 were obtained (Table 1). Strains were stored in 15% (vol/vol) glycerol at -80°C and routinely maintained on YPD (1% yeast extract, 2% peptone, and 2% dextrose; Sigma-Aldrich, USA) and YPL media (1% yeast extract, 2% peptone, and 2% lactate; (Sigma-Aldrich, USA) prior to the experiments.

Table 1. *Candida albicans* Strains Used in This Study

Strain	Genotype/Description	Source, (19)
CA1395 (ICL1/ICL1)	RM1000: ura3Δ: λimm434 ura3Δ: λimm434, his1Δ: hisG his1Δ: hisG, ICL1/ICL1	Barelle et al., 2006.
CA 510 (ICL1/icl1)	RM1000:ura3:λimm434 ura3ΔΔim hisG his1Δ: hisG; icl1: loxP-HIS1loxP ICL1	Barelle et al., 2006
CA 517 (icl1/icl1)	RM1000icl1: loxP-HIS1-loxP/icl1:loxP-URA3-loxP.	Barelle et al., 2006

3.2. Biofilm Formation

Biofilm cultivation of the strains was performed using the silicone elastomer protocol in 6-well plates and the 96-well plate method (20, 21) with slight modification. Strains were propagated in YPD, YPL (Paisley, UK), and RPMI 1640 media inoculated with single colony cells from overnight-grown stock culture, in an orbital shaker at 200 rpm and 35°C. The overnight grown wildtype, single-knockout, and double-knockout *C. albicans* cells were harvested by centrifuging at 3,000 rpm for 5 minutes at 4°C (3×). The cells were standardized using the spectrophotometer to OD600 of 0.1. Next, 100 μL of the standardized inoculum was pipetted into the selected wells and incubated for various time intervals, depicting their developmental growth phases (6, 24, and 48 hours) at 37°C. This experiment was performed in 2 - 4 replicates.

Biofilm cultivation on cellulose filter paper (15 mm in diameter, 0.2 μm pore size) was carried out using flat-bottomed 6-well plates. Strains were inoculated into 100 mL of YPL, YPD, and RPMI 1640 supplemented broths and incubated overnight in an orbital shaker at 35°C and 200 rpm. After the centrifugation of the previously grown primary culture, the cell pellets were resuspended in sterile 10 mL 0.15 M PBS and cell density was standardized to 1×10^7 CFU/mL. Next, 2 mL of each inoculum was added to 6-well plates containing sterilized 15 mm filter membranes, and incubated for 90 minutes at 37°C for adhesion of cells to the membranes, without shaking. After the adhesion phase, the medium was carefully aspirated and the membranes were gently washed in 2 mL sterile 0.15 MPBS twice to remove non-adherent cells. The membranes were carefully transferred with a sterile forceps into new 6-well plates containing 2 mL of YPD and YPL and supplemented with RPMI-1640. The plates were incubated for different time intervals (6, 24, and 48 hours) at 37°C, representing the early, intermediate, and mature phases, respectively, of biofilm formation.

3.3. MTT Reduction Assay

A colorimetric MTT reduction assay was performed as described by Hawser and Douglas in 1995 (22). Stock solution (0.5%, 5 mg/mL⁻¹) was prepared by dissolving 5 mg of MTT salt into 1 mL of sterile PBS. Working solution was prepared by diluting the stock 1: 10 (V/V).

3.4. Antifungal Susceptibility

For antifungal susceptibility testing of sessile cells, biofilms that formed on the microtiter plates at the various time intervals (6, 24, and 48 hours) were challenged with antifungal drugs. The media were aspirated off and gently washed twice with sterile PBS, then 100 μL of YPD and YPL

broth and RPMI 1640 medium containing serially diluted concentrations of antifungals (fluconazole 256 $\mu\text{g}/\text{mL}$ and amphotericin B 16 $\mu\text{g}/\text{mL}$) was added and the plates were incubated for another 24 hours at 37°C. The MTT reduction assay at 405 nm was performed as described (22). The experiment was performed in 2 - 4 replicates.

3.5. Biofilm Compound Light Microscopy

The developmental stages were examined using a compound light. At different time intervals, the biofilms grown in lactate medium were repeatedly washed with PBS and viewed at 20 \times magnification.

3.6. Biofilm Scanning Electron Microscopy (SEM)

The biofilms were fixed using McDowell-Trump fixative on cellulose filter paper. The membranes were serially dehydrated by ethanol washes and immersed in hexamethyldisilazane (HMDS) (Sigma-Aldrich, USA). After drying, the dehydrated substrates were mounted on the stub. The studs were sputter-coated with gold and palladium (Au/Pd 60/40).

3.7. Cell Wall Polysaccharide Isolation and Composition

Sessile cell soluble extracellular polysaccharides, insoluble extracellular polysaccharides, and intracellular polysaccharides were extracted using 1 M NaOH. Into all of the tubes containing sycamore extracellular polysaccharides (SEPS), insoluble extracellular polysaccharides (IEPS), and intracellular polysaccharides (IPS), 5 mL of absolute ethanol was added, then the tubes were incubated at -20°C for 30 - 60 minutes. All tubes were centrifuged and washed twice with pre-chilled 75% ethanol. The carbohydrate content of each fraction was measured using the phenol-sulfuric acid method, and the results were normalized to a standard curve.

3.8. Beta-1, 3-Glucan Measurement

The matrix glucan was measured using a limulus lysate-based assay as previously described by Nett et al. (14). Biofilms were dislodged and samples were sonicated for 5 minutes at 7 W in PBS, then centrifuged 3 \times at 10,000 rpm for 5 minutes at 4°C to separate the cells from the soluble extracellular polysaccharide with the matrix material. Beta-1,3-glucan was measured using the Glucatell (1,3)- β -D-glucan detection reagent kit.

3.9. RNA Isolation and RT-PCR Expression Analysis

At each developmental stage, the biofilms were washed 3 \times with PBS. TRI reagent was used for RNA extraction. Pre-chilled chloroform was added for separation, and 500 μL of pre-chilled isopropanol was added to the clear aqueous upper part for precipitation. The supernatant was removed and the resulting pellets were washed with 75% ethanol and resuspended in 40 μL of dH_2O . Complementary DNA was generated from the RNA using a Tetro cDNA synthesis kit according to the manufacturer's instructions. Expression levels of the desired genes were quantified using light-cycle 480 SYBR green kits according to the manufacturer's instructions, with a small amount of optimization. Reactions were run at denaturation for 15 seconds and at melting temperature for 15 seconds, with an extension time of 30 seconds for approximately 40 cycles (Table 2) (23).

Table 2. Primers Used for qRT-PCR

Primer	Nucleotide Sequence (5' - 3')	Target mRNA	Product Size
CaFKS1		<i>CaFKS1</i>	169
F	CACTGATTGACCGTTGGTG		
R	TGCTTGCCAATGAGAAACTG		
CaERG11		<i>CaERG11</i>	208
F	ATGGGGTTGCCAATGTTATG		
R	TTCITTTGAGCAGCATCACG		
CaCDR2		<i>CaCDR2</i>	200
F	CCCAAGGTCAATTGGGTATG		
R	CAGCGACTCCAACAATAGCA		
CaACT1		<i>CaACT1</i>	174
F	GGTGATGAAGCCCAATCCAA		
R	GGTGATGAAGCCCAATCCAA		

3.10. Statistical Analyses

Analyses were performed using SPSS 17.0 for Windows. One-way ANOVA was performed to analyze the differences among multiple means. According to the tests of homogeneity of variances, Bonferroni-Dunn was carried out for post-hoc multiple comparisons. P values of < 0.05 were considered statistically significant.

4. Results

4.1. Biofilm Formation is Independent of Isocitrate Lyase

The *icl1/icl1* mutants formed biofilms, as revealed by MTT quantification, at each developmental stage. Interestingly, *ICL1/icl1* and *icl1/icl1* cells were metabolically active at

a similar level to the wildtype cells in the presence and absence of glucose. **Figure 2A - 2C** depict a significantly ($P < 0.05$) higher degree of formation in glucose and lactate media in the wildtype and *icl1/icl1* strains than in *ICL1/icl1*. However, metabolic activity increased with maturation in all strains. There was no significant difference among the three strains on RPMI 1640. At maturity, the strains' growth displayed no obvious differences on YPL and YPD. This result indicates that *ICL1* is not essential for growth under these conditions.

4.2. Resistance Phenotype is Independent of Isocitrate Lyase

We investigated *ICL*'s impact on *C. albicans* biofilm resistivity. Biofilms at each developmental phase on a non-carbohydrate medium (lactate) were treated with 256 $\mu\text{g}/\text{mL}$ of fluconazole and 16 $\mu\text{g}/\text{mL}$ of amphotericin B based on $\text{SMIC}_{50\%}$. **Figure 3A - 3C** show that the reference, *ICL1/icl1*, and *icl1/icl1* strains exhibited high resistance to fluconazole at the 256 $\mu\text{g}/\text{mL}$ concentration at all stages (as well as in the YPD and RPMI media; data not shown). Growth was characterized by high metabolic activity that did not deviate significantly from untreated biofilms. As seen in **Figure 3B - 3C**, a 20% inhibitory effect was conserved with 16 $\mu\text{g}/\text{mL}$ amphotericin B on *ICL1/icl1* and *icl1/icl1* biofilms at 6 hours. However, resistance built up at the intermediate and mature phases, as seen in **Figure 3B - 3C**. In addition, resistance increased with metabolic activity regardless of the supporting medium and the in vitro materials used. This result indicates that the glyoxylate cycle is not essential for resistance to these antifungal drugs.

4.3. Biofilms Grow in Three Developmental Stages

Our results confirmed that biofilm development progresses in three distinct stages. The early phase (**Figure 4A - 4C**) showed free-floating cells attached to the substratum and to each other in microcolonies. The intermediate phase (**Figure 4D - 4F**) shows active replication, evident through increased numbers of microcolonies, with heterogeneous communities consisting of hyphae and pseudohyphae in the wildtype cells (**Figure 4D**). Filamentous morphogenesis was absent in the mutant biofilms (**Figure 4E - 4I**).

4.4. Isocitrate Lyase (*ICL*) Alters Morphogenesis

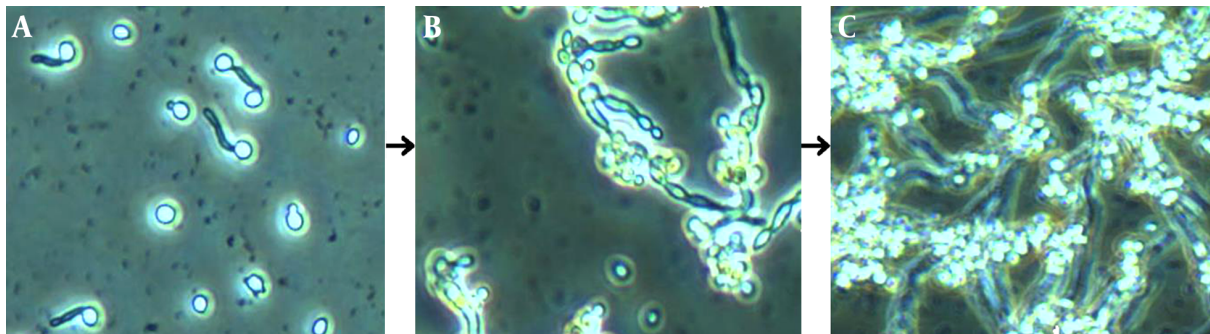
In an attempt to visualize the role of *ICL* on biofilm structural organization and morphology during challenges with antifungal drugs, mature biofilms of the reference and reconstructed mutants on cellulose membranes were treated with 256 $\mu\text{g}/\text{mL}$ of fluconazole, then examined under SEM and compared to untreated biofilms.

Selected concentrations were based on generated susceptibility testing data. The reference strain-treated biofilm (**Figure 5A**) conformed to previous descriptions [33]. This community presented a highly heterogeneous assemblage, with visible pseudohyphae, hyphae, and blastospores encased within the ECM and divided into two distinct layers. Blastospores were more concentrated and tightly packed at the basal region, while the upper region consisted of pseudohyphae and true hyphae networks. Untreated wildtype biofilms (**Figure 5B**) exhibited substantially less hyphae growth, consisting mostly of budding, densely packed, clustered yeast cells. Hyphae growth was incapacitated and defective in the reconstructed mutants, with no visible bilayer in either the treated or the untreated biofilms. The treated *ICL1/icl1* strain seen in **Figure 5C** showed resistance, as indicated by the steadiness of metabolic activity and the detectable cluster of yeast cells in the basal region. The untreated biofilm seen in **Figure 5D** was characterized by a mass cluster of viable cells with defective hyphae growth. The *icl1/icl1* strain (**Figure 5E**) exhibited the same basal composition as *ICL1/icl1*, but with smaller and denser adhered, mature, and budding blastospores. The generated images suggest that *ICL1* influences morphogenesis under these conditions.

4.5. ECM β -1, 3-Glucan is Dependent on Cell Wall Polysaccharides

We designed a hypothesis to answer whether sessile cells generate glucan using alternative generated hexoses in the absence of the glyoxylate pathway in relative proportion to when glyoxylate is present. Also, we further exploited the extent of glucan defenses against treatment at each developmental stage. **Table 3** reveals that the cell wall carbohydrates of treated and untreated strains increased with time. Compared to the wildtype cells, hexose accumulation in untreated and treated *icl1/icl1* and *ICL1/icl1* was not impaired despite the absence of *ICL*. These data indicate that hexoses were synthesized through other active pathways. Synthesis was more amplified in treated than in untreated biofilms, and the increment was proportional to time.

Sequestration activity through matrix β -1, 3-glucan encoded by the *FKS1* gene mediates tolerance to azole drugs [40, 41]. To determine the β -1, 3-glucan concentration in the matrix, *C. albicans* wildtype, *ICL1/icl1*, and *icl1/icl1* biofilms on YPL medium were measured using a GlucateLL (1, 3)- β -D-glucan detection reagent kit based on limulus lysate. **Figure 6A - 6B** show that the increase was significantly higher in wildtype and *icl1/icl1* compared to *ICL1/icl1* at all stages. At the mature stages, *ICL1/ICL1* showed a greater rate than the mutant strain, and the *icl1/icl1* glucan level was moderately higher than that of *ICL1/icl1*. After treatment, as de-

Figure 1. Inverted Microscopy Images of *C. albicans* Biofilms at Different Growth Stages on RPMI 1640 Medium

These images depict biofilm formation on a polystyrene surface under static conditions through the three developmental phases. A, Growing predominantly as yeast cells, attachment of the cells to the potential growth material and to each other was observed; B, metabolic activity increased with cellular density in correlation with the duration of cultivation. This image shows cells at the maturation phase; C, Microcommunities became heterogeneous and clustered. Apparent production and visible accumulation of slime extracellular matrix (ECM) enclosing the sessile yeast and filamentous cells, which increased with maturity, was observed.

picted in Figure 6B, glucan levels were significantly higher ($P > 0.05$) in the wildtype at 6 and 24 hours. These results indicate that the concentrations were significantly higher in treated than in untreated biofilms. All of the strains synthesized β -1, 3-glucan at different rates. A direct relationship was observed between hexose and β -1, 3-glucan because as carbohydrate increased, glucan also increased in the matrix, confirming that concentration in the ECM is dependent on the amount of hexose present. We can say that modulation of ICL did not lower or halt synthesis because hexoses were produced independently. Evidence of resistance, tolerance with maturation, resistance to drugs, and the synthesis of glucan signifies glucan's major impact on the phenotype. This research showed that metabolism through the preferred alternative glyoxylate pathway is not a specific regulator of the biofilm resistance phenotype.

4.6. Transcript Profile of Associated Resistance Genes Regulated by Isocitrate Lyase

We investigated the extent of ICL's regulatory role on *FKSI*, *ERG11*, and *CDR2* at the mRNA expression level using real-time qPCR. *ACT1* was used as a housekeeping gene. The expression profiles of *ICL1/icl1* and *icl1/icl1* were compared to that of the wildtype strain. Figure 7A shows that the expression level of *FKSI* in the mutants was downregulated compared to the wildtype. *FKSI* transcript levels were relatively high at the intermediate phase in the mutants, although no fold to the wildtype was suggested, and expression decreased at maturity. Expression of *ERG11* in *icl1/icl1* regressed over time, unlike that of *ICL1/icl1*, which increased at the intermediate stage and regressed at maturity (Figure 7B). The drug efflux-pump level was also reduced with maturation. The *ICL1/icl1CDR2* level was higher than that of

Table 3. Comparison of Carbohydrate Concentrations of Biofilm Sessile Cell Walls Before and After Treatment

<i>Candida albicans</i> strain	Untreated, $\mu\text{g/ml}$	Treated, $\mu\text{g/ml}$	Correlation With ECM Glucan
<i>CaICL1/icl1</i>			
Increase with time	Lower concentration	Higher concentration	
hours	49.4 \pm 0.0	49.3 \pm 0.6	+
hours	97.0 \pm 0.0	98.0 \pm 0.1	+
hours	126.0 \pm 0.5	125.2 \pm 0.1	+
<i>CaICL1/icl1</i>			
Increase with time	Lower concentration	Higher concentration	
hours	26.0 \pm 0.3	31.03 \pm 1.0	+
hours	22.5 \pm 0.6	65.1 \pm 0.2	+
hours	32.2 \pm 0.3	141.0 \pm 0.2	+
<i>Caicl1/icl1</i>			
Increase with time	Lower concentration	Higher concentration	
hours	19.6 \pm 0.0	23.3 \pm 0.6	+
hours	54.0 \pm 0.0	151.0 \pm 0.0	+
hours	46.0 \pm 0.0	149 \pm 0.6	+

the wildtype at the early phase and decreased to reference levels at maturity. Overall, the transcript levels of the studied genes were downregulated to the wildtype, as shown in Figure 7C. Therefore, our data show that ICL exerts a substantial regulatory effect on *FKSI*, *ERG11*, and *CDR2* expression.

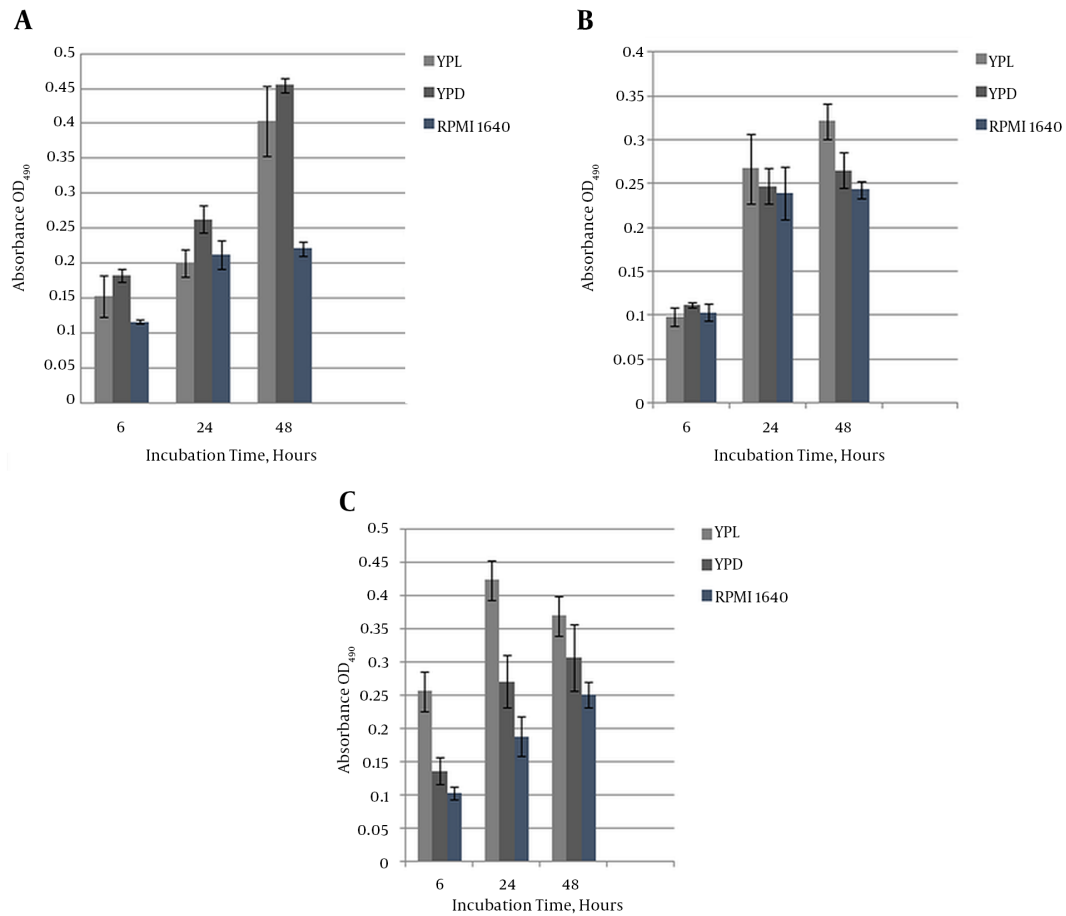


Figure 2. A, The chart represents the average metabolic activity OD of *C. albicans* wildtype biofilms on YPL, YPD, and RPMI 1640 media, measured with the MTT assay at each developmental stage (early, intermediate, and maturation). The results are representative of three independent experiments. Absorbance is plotted against growth intervals (time); B, Heterozygous CalCl1/icl1 mutant biofilm on YPL, YPD, and RPMI 1640 media. Formation at early, intermediate, and maturation stages. The results are representative of three independent experiments. Absorbance is plotted against growth intervals (time). Independent experiments were performed in triplicate; C, Homozygous CalCl1/icl1 mutant biofilm on YPL, YPD, and RPMI 1640 media. Formation is shown at the early, intermediate, and maturation stages. The results are representative of three independent experiments. Absorbance is plotted against growth intervals (time). Independent experiments were performed in triplicate.

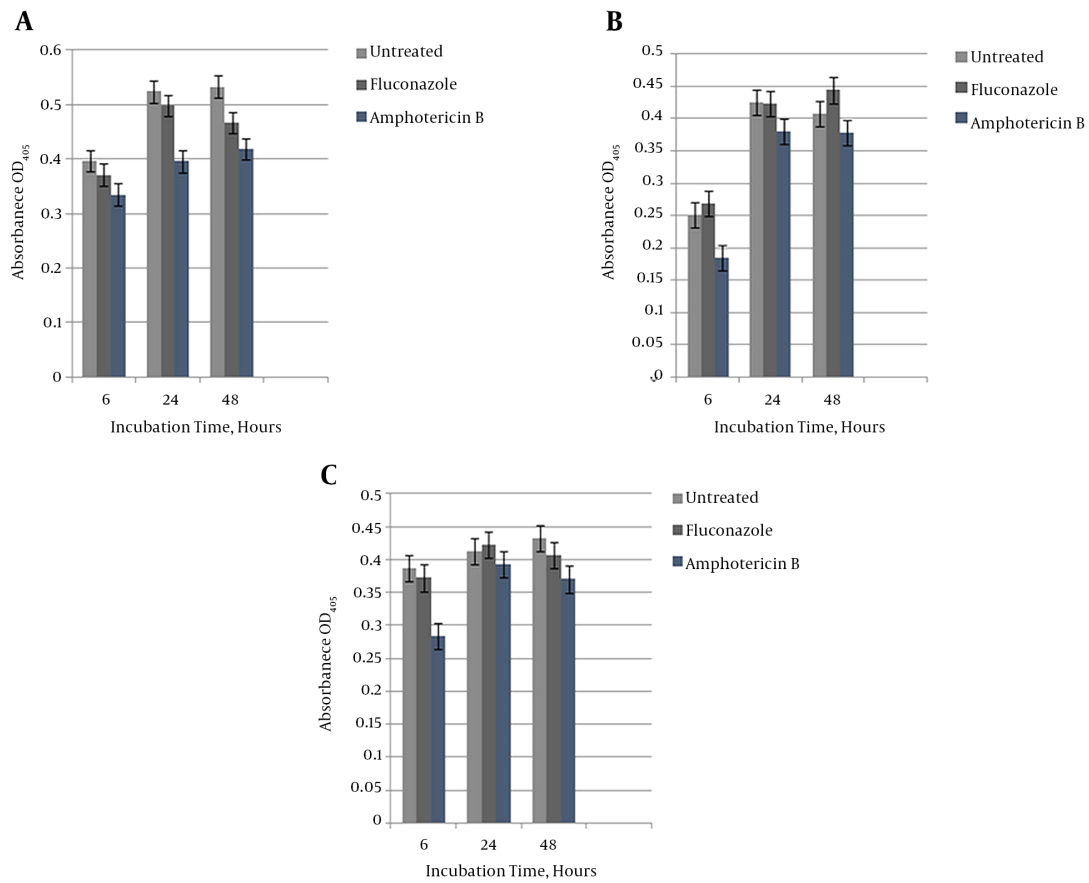


Figure 3. A, *C. albicans* wildtype susceptibility testing with fluconazole 128 $\mu\text{g}/\text{mL}$ and amphotericin B 16 $\mu\text{g}/\text{mL}$ on lactate-containing medium. ANOVA was carried out for the statistical analysis to calculate the significant difference at each developmental level; B, Heterozygous *CaCL1/icl1* mutant susceptibility testing with fluconazole 128 $\mu\text{g}/\text{mL}$ and amphotericin B 16 $\mu\text{g}/\text{mL}$ on lactate-containing medium. ANOVA was carried out for the statistical analysis to calculate the significant difference at each developmental level. Independent experiments were performed in triplicate.

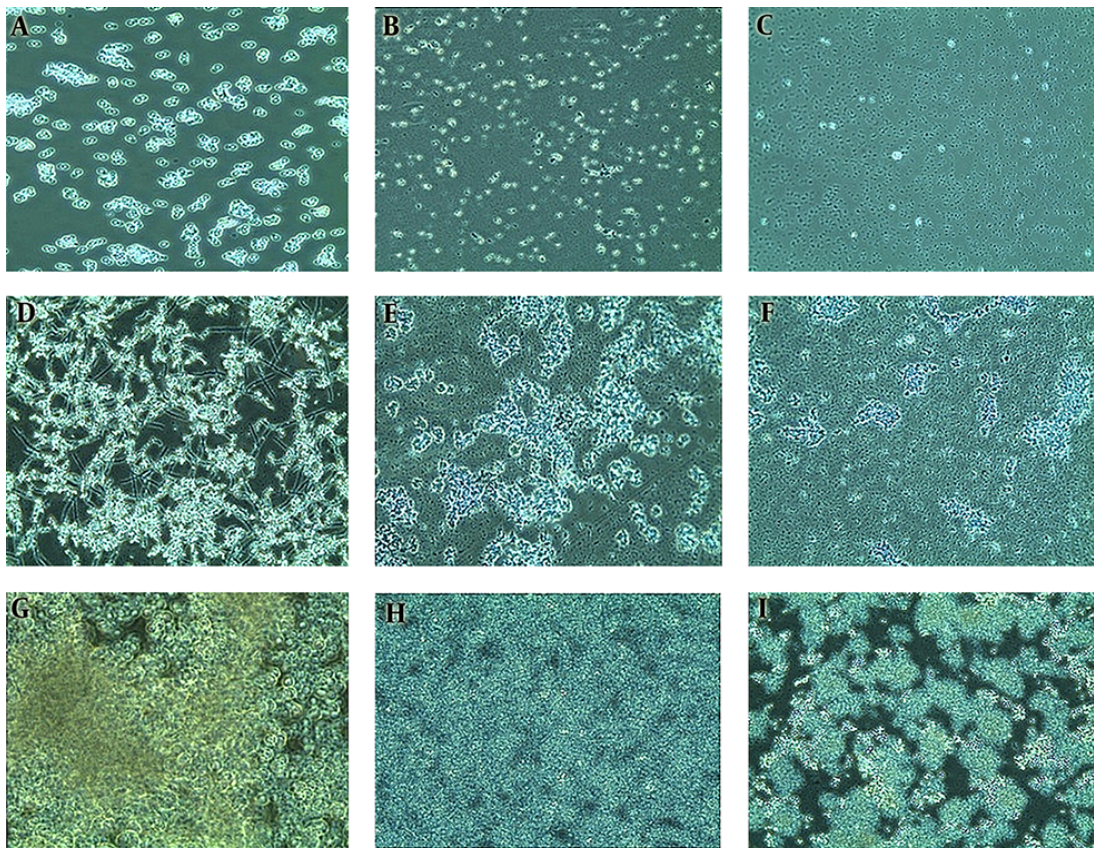


Figure 4. Developmental Stages of Biofilms

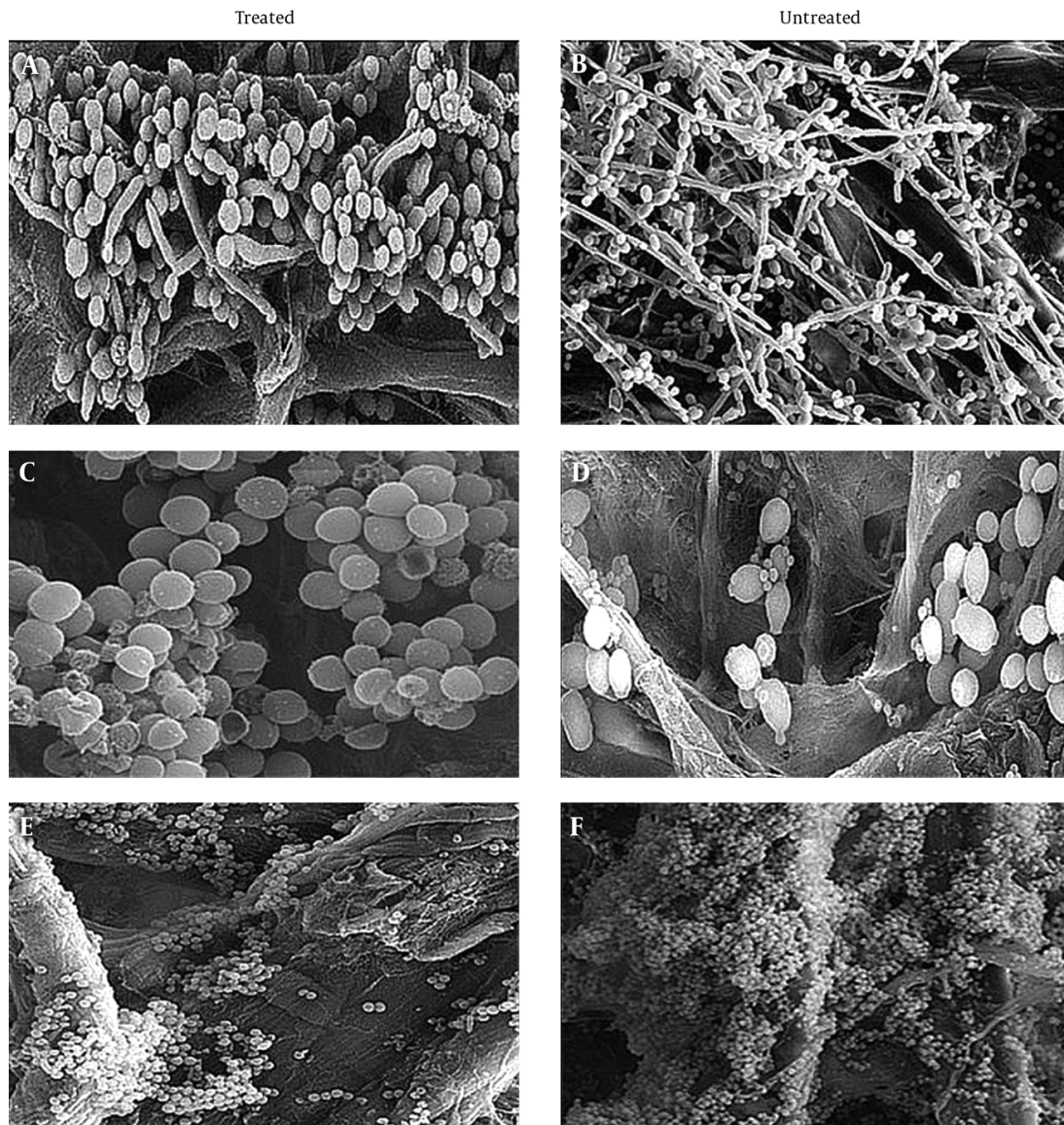


Figure 5. SEM images of reference and knockout strain biofilms at maturity, before and after treatment. Biofilms were cultured for 48 hours at 37°C under static conditions in YPL medium and visualized at 500 × magnification. A, Treated wildtype ICL1/ICL1; B, untreated wildtype ICL1/ICL1; C, treated ICL1/ict1; D, untreated ICL1/ict1; E, treated ict1/ict1, and F, untreated ict1/ict1. Images have been reconstructed to permit clear viewing.

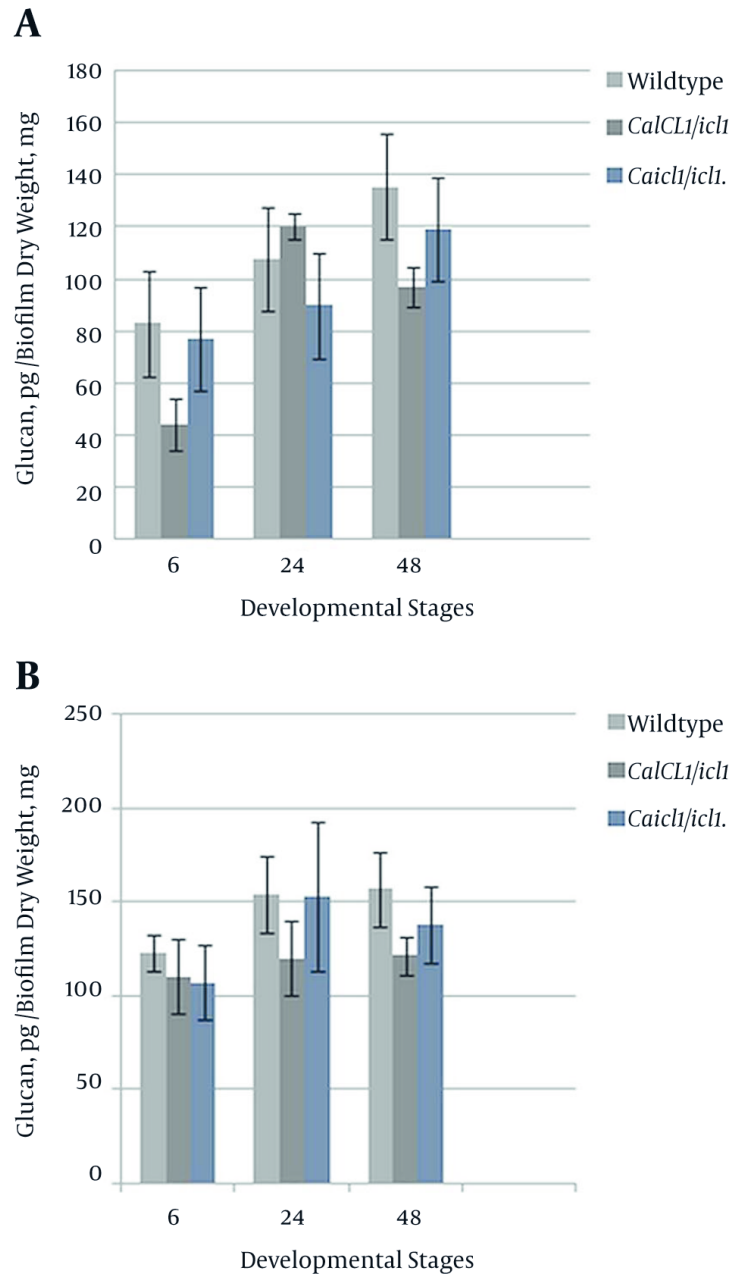


Figure 6. A, Quantification of β -1, 3-glucan present in the ECM of wildtype and mutant biofilms not treated with fluconazole at the early, intermediate, and mature phases, respectively; B, Quantification of β -1, 3-glucan present in the ECM of the wildtype and mutant biofilms treated with 128 μ g/ml fluconazole at the early, intermediate, and mature phases, respectively.

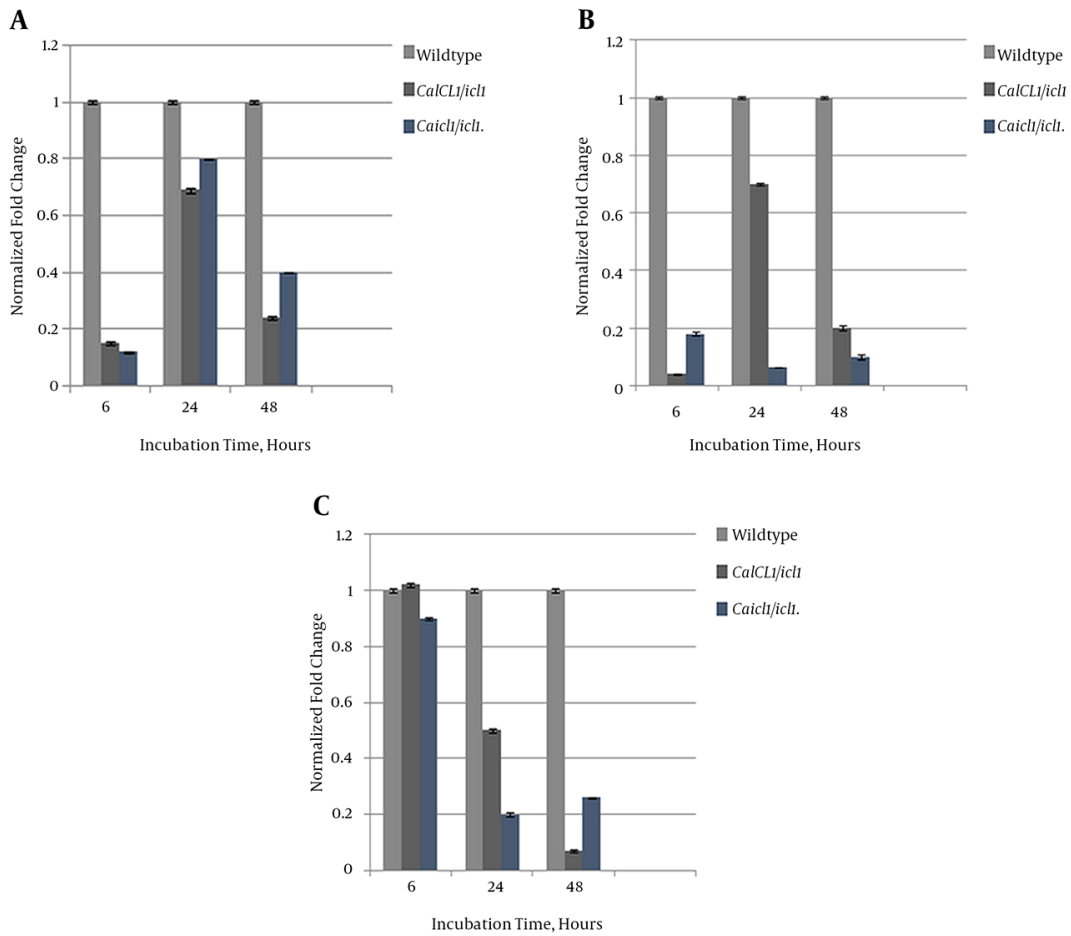


Figure 7. A, Comparative Relative Transcriptional Expression of *FKS1*; Results were normalized to the internal control *CaACT1*; B, Comparative relative transcriptional expression of *ERG11*. Results were normalized to the housekeeping gene *CaACT1*; C, Comparative relative transcriptional expression of *CDR2*. Results were normalized to the internal control *CaACT1*.

5. Discussion

Metabolic flexibility aids *C. albicans* in establishing infections (19, 24, 25). We examined the possible roles of ICL1, a major glyoxylate-synthesizing enzyme, in the distinctive traits of biofilms. Biofilm formation by ICL1/*icl1* and *icl1*/*icl1* showed a partial impact of ICL, as metabolic activity remained high. The continual growth of ICL1 mutants on non-fatty-acid compounds showed that glyoxylate is not the sole pathway capable of synthesizing C₄ molecules for gluconeogenesis, suggesting the presence of similar derivatives and other catabolic pathways. The glyoxylate cycle is preferred because it consumes less energy; however, it can be bypassed in the presence of glucose, farnesol, lactate, malic acid, and succinic acid. Moreover, glucose and fatty acids are more energetically favorable and thus their presence represses lactate assimilation (19, 26).

Lactate, malic acid, and succinic acid derived from pyruvate can be oxidized to oxaloacetate through the pyruvate dehydrogenase pathway. This supports the observation that ICL1/*icl1* and *icl1*/*icl1* are able to form extensive biofilms in lactate-containing media. The low assimilation observed in ICL1/*icl1* (Figure 2B), later compensated by a rapid growth at the intermediate phase until the matured stage, could be due to incomplete dependence on the pyruvate decarboxylase pathway because of ICL1 allele partial expression; the glyoxylate pathway is preferred to other alternative pathways until the depletion of the precursor. The significant growth of biofilms on RPMI 1640 medium suggests that ICL does not affect their formation. A possible rationale is that growth on lactate may enhance *C. albicans* survival and metabolic activity, influencing biofilm growth through combinatorial synthesis of limited carbon. This supports that multiple assimilation mechanisms are used simultaneously to maintain their signature resistance (27). Metabolic robustness supports growth, thereby promoting resistance, which increases with maturation and metabolic activity.

The resistance phenotype expressed at each formation stage increased with maturation. The evidence showcased the insignificant role of ICL in the resistance of sessile cells, although it may be partially involved in the early-phase metabolic shift, as shown in Figure 3. However, there was no significant association between isocitrate lyase and clinical resistance, signifying that ICL is not a sole determinant of this characteristic. The *C. albicans* biofilm resistance phenotype signature and virulence potential for initiating infections was not impaired; in fact, it was enhanced by the high metabolic action that increased with time. Absence of ICL may activate and deactivate other genes that function in resistance acquisition, as observed in *zap1*/*zap1* mutants (28). For that reason, a conclusion was

reached that ICL deletion may upregulate other resistance mechanisms that compensate for its unavailability. Developmental images define the complexity of biofilms and identify three distinct growth phases. Filamentous growth is a prominent feature of biofilms, and hyphae growth incapacitation in the absence of ICL to a substantial extent suggests that there is lower proliferation in tissues and less establishment of infections through the dissemination of yeast cells. Furthermore, attenuation of filamentous growth confirms ICL as a promoter of hyphae morphogenesis (24, 26, 29, 30).

The roles of modifying proteins Bgl2, Phr1, and Xog1 have been recently reported to mediate glucan delivery to the matrix through a controlled channel from the cell wall, along with depletion signaling. Our results showed the activity of the glucan synthase pathway and of β -1, 3-glucan in the ECM, depicting the activity of delivery mechanisms (30). Lower accumulation at the early phase may be due to high energy consumption by the survival and replication processes. At the mature phases, the significant amplification may perhaps be attributed to energy conservation and upregulation of mechanisms that mediate survival. It could also be a reflection of stable β -1, 3-glucan due to lower sequestration activity as a result of other stage-specific mechanisms of resistance. Gene expression profiling revealed a substantial effect of ICL on the mRNA of the resistance genes, suggesting that resistivity tends toward genotypic variation.

Glucan synthase-encasing gene expression explains the continual synthesis of β -1, 3-glucan as observed in the constructed mutants. Previous works have shown that *ERG11* transcripts are higher in young biofilms, which was supported by the findings of this study (31, 32). Upregulation of *ERG11* at the early and intermediate stages suggests that its role is streamlined to certain stages, and its expression indicates a response to fluconazole treatment through sterol accumulation and mutation. High *ERG11* expression in ICL1/*icl1* suggests that ICL is needed for *ERG11* functionality. However, resistance was maintained, suggestive of influences by other mechanisms. The role of efflux-pump genes has been addressed (31, 33, 34). These genes are responsible for the expulsion of drugs from cells. The results of the present study revealed the function of *CDR2* to be early-phase-specific. Nevertheless, resistance was exhibited at all stages, suggestive of other genetic influences that are yet to be identified. Thus, ICL may be a part of the synergistic interactions and mechanisms that mediate biofilm resistance phenotypes.

Biofilm formation by *C. albicans* ICL heterozygous and homozygous mutants was found to not be regulated by ICL, as metabolic activity remained high, suggesting that ICL is a negative regulator for other synthesizing enzymes

and pathways, thereby advancing the cell's growth and homeostasis. The resistance phenotype was expressed at each formation stage, increasing with maturation. True hyphae morphogenesis impairment indicates filamentous growth as a prominent feature of biofilms, regulated by the preferred non-fermentable carbohydrate-absorption pathway.

Acknowledgments

The authors would like to sincerely thank the ministry of higher education of Malaysia and the Universiti Sains Malaysia (USM) for the fundamental research grant scheme (FRGS) funding (203/CIPPT/11242, <http://jpt.mohe.gov.my>), which supported this work. The authors would also like to acknowledge the Universiti Sains Malaysia for the research university individual (RUI) grants (No: 1001/CIPPT/812196 and No: 304/CIPPT/6313241).

Footnote

Authors' Contribution: Study concept and design, Doblin Sandai, Leslie Than Thian Lung, Muhammad Yunus, and Rafeezul Mohamed; analysis and interpretation of data, Doblin Sandai, Muhammad Amir Yunus, Oluwaseun Ayodeji Ishola, Ting Seng Yeat, Yasser Tabana, and Mowaffaq Adam Ahmaed; drafting and reviewing of the manuscript, Oluwaseun Ayodeji Ishola, Doblin Sandai, and Muhammad Amir Yunus; critical revision of the manuscript for important intellectual content, Doblin Sandai, Leslie Than Thian Lung, Muhammad Yunus, Rafeezul Mohamed, Oluwaseun Ayodeji Ishola, Ting Seng Yeat, Yasser Tabana, and Mowaffaq Adam Ahmed.

References

- Jabra-Rizk MA, Falkler WA, Meiller TF. Fungal biofilms and drug resistance. *Emerg Infect Dis*. 2004;**10**(1):14–9. doi: [10.3201/eid1001.030119](https://doi.org/10.3201/eid1001.030119). [PubMed: [15078591](https://pubmed.ncbi.nlm.nih.gov/15078591/)].
- Calderone R, Gow NA. Host recognition by Candida species. Washington, DC: Candida and candidiasis ASM Press; 2002. pp. 67–86.
- Sardi JC, Scorzoni L, Bernardi T, Fusco-Almeida AM, Mendes Giannini MJ. Candida species: current epidemiology, pathogenicity, biofilm formation, natural antifungal products and new therapeutic options. *J Med Microbiol*. 2013;**62**(Pt 1):10–24. doi: [10.1099/jmm.0.045054-0](https://doi.org/10.1099/jmm.0.045054-0). [PubMed: [23180477](https://pubmed.ncbi.nlm.nih.gov/23180477/)].
- Ramage G, Rajendran R, Sherry L, Williams C. Fungal biofilm resistance. *Int J Microbiol*. 2012;**2012**:528521. doi: [10.1155/2012/528521](https://doi.org/10.1155/2012/528521). [PubMed: [22518145](https://pubmed.ncbi.nlm.nih.gov/22518145/)].
- Brown A, Argimon S, Gow N. Signal transduction and morphogenesis in Candida albicans. USA: Springer; 2007. pp. 167–94.
- Ramage G, Saville SP, Thomas DP, Lopez-Ribot JL. Candida biofilms: an update. *Eukaryot Cell*. 2005;**4**(4):633–8. doi: [10.1128/EC.4.4.633-638.2005](https://doi.org/10.1128/EC.4.4.633-638.2005). [PubMed: [15821123](https://pubmed.ncbi.nlm.nih.gov/15821123/)].
- Douglas LJ. Medical importance of biofilms in Candida infections. *Rev Iberoam Micol*. 2002;**19**(3):139–43. [PubMed: [12825991](https://pubmed.ncbi.nlm.nih.gov/12825991/)].
- Pfaller M, Jones R, Messer S, Edmond M, Wenzel R. National surveillance of nosocomial blood stream infection due to Candida albicans: frequency of occurrence and antifungal susceptibility in the SCOPE Program. *Diagn Microbiol Infect Dis*. 1998;**31**(1):327–32. [PubMed: [9597393](https://pubmed.ncbi.nlm.nih.gov/9597393/)].
- Brown GD, Denning DW, Gow NA, Levitz SM, Netea MG, White TC. Hidden killers: human fungal infections. *Sci Transl Med*. 2012;**4**(165):165. doi: [10.1126/scitranslmed.3004404](https://doi.org/10.1126/scitranslmed.3004404). [PubMed: [23253612](https://pubmed.ncbi.nlm.nih.gov/23253612/)].
- Finkel JS, Mitchell AP. Genetic control of Candida albicans biofilm development. *Nat Rev Microbiol*. 2011;**9**(2):109–18. doi: [10.1038/nrmicro2475](https://doi.org/10.1038/nrmicro2475). [PubMed: [21189476](https://pubmed.ncbi.nlm.nih.gov/21189476/)].
- Chandra J, Mukherjee PK, Leidich SD, Faddoul FF, Hoyer LL, Douglas LJ, et al. Antifungal resistance of candidal biofilms formed on denture acrylic in vitro. *J Dent Res*. 2001;**80**(3):903–8. [PubMed: [11379893](https://pubmed.ncbi.nlm.nih.gov/11379893/)].
- Douglas LJ. Candida biofilms and their role in infection. *Trends Microbiol*. 2003;**11**(1):30–6. [PubMed: [12526852](https://pubmed.ncbi.nlm.nih.gov/12526852/)].
- Taff HT, Nett JE, Zarnowski R, Ross KM, Sanchez H, Cain MT, et al. A Candida biofilm-induced pathway for matrix glucan delivery: implications for drug resistance. *PLoS Pathog*. 2012;**8**(8):1002848. doi: [10.1371/journal.ppat.1002848](https://doi.org/10.1371/journal.ppat.1002848). [PubMed: [22876186](https://pubmed.ncbi.nlm.nih.gov/22876186/)].
- Nett JE, Sanchez H, Cain MT, Andes DR. Genetic basis of Candida biofilm resistance due to drug-sequestering matrix glucan. *J Infect Dis*. 2010;**202**(1):171–5. doi: [10.1086/651200](https://doi.org/10.1086/651200). [PubMed: [20497051](https://pubmed.ncbi.nlm.nih.gov/20497051/)].
- Baillie GS, Douglas LJ. Role of dimorphism in the development of Candida albicans biofilms. *J Med Microbiol*. 1999;**48**(7):671–9. doi: [10.1099/00222615-48-7-671](https://doi.org/10.1099/00222615-48-7-671). [PubMed: [10403418](https://pubmed.ncbi.nlm.nih.gov/10403418/)].
- Sardi JC, Almeida AM, Mendes Giannini MJ. New antimicrobial therapies used against fungi present in subgingival sites—a brief review. *Arch Oral Biol*. 2011;**56**(10):951–9. doi: [10.1016/j.archoralbio.2011.03.007](https://doi.org/10.1016/j.archoralbio.2011.03.007). [PubMed: [21676377](https://pubmed.ncbi.nlm.nih.gov/21676377/)].
- Viudes A, Peman J, Canton E, Ubeda P, Lopez-Ribot JL, Gobernado M. Candidemia at a tertiary-care hospital: epidemiology, treatment, clinical outcome and risk factors for death. *Eur J Clin Microbiol Infect Dis*. 2002;**21**(11):767–74. doi: [10.1007/s10096-002-0822-1](https://doi.org/10.1007/s10096-002-0822-1). [PubMed: [12461585](https://pubmed.ncbi.nlm.nih.gov/12461585/)].
- Bink A, Pellens K, Cammue PAB, Thevissen K. Anti-biofilm strategies: how to eradicate Candida biofilms?. *Open Mycol J*. 2011;**5**(1):29–38. doi: [10.2174/1874437001105010029](https://doi.org/10.2174/1874437001105010029).
- Barelle CJ, Priest CL, Maccallum DM, Gow NA, Odds FC, Brown AJ. Niche-specific regulation of central metabolic pathways in a fungal pathogen. *Cell Microbiol*. 2006;**8**(6):961–71. doi: [10.1111/j.1462-5822.2005.00676.x](https://doi.org/10.1111/j.1462-5822.2005.00676.x). [PubMed: [16681837](https://pubmed.ncbi.nlm.nih.gov/16681837/)].
- Chandra J, Mukherjee PK, Ghannoum MA. In vitro growth and analysis of Candida biofilms. *Nat Protoc*. 2008;**3**(12):1909–24. doi: [10.1038/nprot.2008.192](https://doi.org/10.1038/nprot.2008.192). [PubMed: [19180075](https://pubmed.ncbi.nlm.nih.gov/19180075/)].
- Pierce CG, Uppuluri P, Tristan AR, Wormley FL, Mowat E, Ramage G, et al. A simple and reproducible 96-well plate-based method for the formation of fungal biofilms and its application to antifungal susceptibility testing. *Nat Protoc*. 2008;**3**(9):1494–500. doi: [10.1038/nprot.2008.141](https://doi.org/10.1038/nprot.2008.141). [PubMed: [18772877](https://pubmed.ncbi.nlm.nih.gov/18772877/)].
- Hawser SP, Douglas LJ. Resistance of Candida albicans biofilms to antifungal agents in vitro. *Antimicrob Agents Chemother*. 1995;**39**(9):2128–31. [PubMed: [8540729](https://pubmed.ncbi.nlm.nih.gov/8540729/)].
- Green CB, Cheng G, Chandra J, Mukherjee P, Ghannoum MA, Hoyer LL. RT-PCR detection of Candida albicans ALS gene expression in the reconstituted human epithelium (RHE) model of oral candidiasis and in model biofilms. *Microbiology*. 2004;**150**(Pt 2):267–75. doi: [10.1099/mic.0.26699-0](https://doi.org/10.1099/mic.0.26699-0). [PubMed: [14766904](https://pubmed.ncbi.nlm.nih.gov/14766904/)].
- Lorenz MC, Fink GR. The glyoxylate cycle is required for fungal virulence. *Nature*. 2001;**412**(6842):83–6. doi: [10.1038/35083594](https://doi.org/10.1038/35083594). [PubMed: [11452311](https://pubmed.ncbi.nlm.nih.gov/11452311/)].
- Lorenz MC, Bender JA, Fink GR. Transcriptional response of Candida albicans upon internalization by macrophages. *Eukaryot Cell*. 2004;**3**(5):1076–87. doi: [10.1128/EC.3.5.1076-1087.2004](https://doi.org/10.1128/EC.3.5.1076-1087.2004). [PubMed: [15470236](https://pubmed.ncbi.nlm.nih.gov/15470236/)].

26. Piekarska K, Mol E, van den Berg M, Hardy G, van den Burg J, van Roermund C, et al. Peroxisomal fatty acid beta-oxidation is not essential for virulence of *Candida albicans*. *Eukaryot Cell*. 2006;5(11):1847-56. doi: [10.1128/EC.00093-06](https://doi.org/10.1128/EC.00093-06). [PubMed: [16963628](https://pubmed.ncbi.nlm.nih.gov/16963628/)].
27. Sandai D, Yin Z, Selway L, Stead D, Walker J, Leach MD, et al. The evolutionary rewiring of ubiquitination targets has reprogrammed the regulation of carbon assimilation in the pathogenic yeast *Candida albicans*. *MBio*. 2012;3(6) doi: [10.1128/mBio.00495-12](https://doi.org/10.1128/mBio.00495-12). [PubMed: [23232717](https://pubmed.ncbi.nlm.nih.gov/23232717/)].
28. Nobile CJ, Nett JE, Hernday AD, Homann OR, Deneault JS, Nantel A, et al. Biofilm matrix regulation by *Candida albicans* Zap1. *PLoS Biol*. 2009;7(6):1000133. doi: [10.1371/journal.pbio.1000133](https://doi.org/10.1371/journal.pbio.1000133). [PubMed: [19529758](https://pubmed.ncbi.nlm.nih.gov/19529758/)].
29. Ramirez MA, Lorenz MC. Mutations in alternative carbon utilization pathways in *Candida albicans* attenuate virulence and confer pleiotropic phenotypes. *Eukaryot Cell*. 2007;6(2):280-90. doi: [10.1128/EC.00372-06](https://doi.org/10.1128/EC.00372-06). [PubMed: [17158734](https://pubmed.ncbi.nlm.nih.gov/17158734/)].
30. Nett J, Lincoln L, Marchillo K, Massey R, Holoyda K, Hoff B, et al. Putative role of beta-1,3 glucans in *Candida albicans* biofilm resistance. *Antimicrob Agents Chemother*. 2007;51(2):510-20. doi: [10.1128/AAC.01056-06](https://doi.org/10.1128/AAC.01056-06). [PubMed: [17130296](https://pubmed.ncbi.nlm.nih.gov/17130296/)].
31. Kuhn DM, George T, Chandra J, Mukherjee PK, Ghannoum MA. Antifungal susceptibility of *Candida* biofilms: unique efficacy of amphotericin B lipid formulations and echinocandins. *Antimicrob Agents Chemother*. 2002;46(6):1773-80. [PubMed: [12019089](https://pubmed.ncbi.nlm.nih.gov/12019089/)].
32. Nailis H, Vandenbosch D, Deforce D, Nelis HJ, Coenye T. Transcriptional response to fluconazole and amphotericin B in *Candida albicans* biofilms. *Res Microbiol*. 2010;161(4):284-92. doi: [10.1016/j.resmic.2010.02.004](https://doi.org/10.1016/j.resmic.2010.02.004). [PubMed: [20170727](https://pubmed.ncbi.nlm.nih.gov/20170727/)].
33. Ramage G, Bachmann S, Patterson TF, Wickes BL, Lopez-Ribot JL. Investigation of multidrug efflux pumps in relation to fluconazole resistance in *Candida albicans* biofilms. *J Antimicrob Chemother*. 2002;49(6):973-80. [PubMed: [12039889](https://pubmed.ncbi.nlm.nih.gov/12039889/)].
34. Watamoto T, Samaranayake LP, Egusa H, Yatani H, Seneviratne CJ. Transcriptional regulation of drug-resistance genes in *Candida albicans* biofilms in response to antifungals. *J Med Microbiol*. 2011;60(Pt 9):1241-7. doi: [10.1099/jmm.0.030692-0](https://doi.org/10.1099/jmm.0.030692-0). [PubMed: [21474609](https://pubmed.ncbi.nlm.nih.gov/21474609/)].